



Scholars Research Library

Der Pharma Chemica, 2015, 7(9):354-367
(<http://derpharmachemica.com/archive.html>)



ISSN 0975-413X
CODEN (USA): PCHHAX

Effect of 1,5-dibenzyl-1H-pyrazolo[3,4-d]pyrimidine-4(5H)-thione on inhibition of mild steel corrosion in 1M HCl

Y. El Ouadi¹, M. Elfal², A. Bouyanzer¹, H. Elmsellem^{1*}, Y. Ramli³, E.M. Essassi², N. Lahhit¹, A. Aouniti¹, A. Chetouani^{1,4} and B. Hammouti¹

¹Laboratoire de Chimie Appliquée et environnement (LCAE-URAC18), Faculté des Sciences, 60000 Oujda, Morocco

²Laboratoire de Chimie Organique Hétérocyclique, URAC 21, Pôle de Compétences Pharmacochimie, Université Mohammed V, Faculté des Sciences, Av. Ibn Battouta, Rabat, Morocco

³Medicinal Chemistry Laboratory, Faculty of Medicine and Pharmacy, Mohammed V, University-Rabat, Morocco

⁴Laboratoire de chimie physique, Centre Régionale des Métiers de l'Éducation et de Formation "CRMEF", Région de l'Orientale, Oujda, Morocco

ABSTRACT

The inhibition effect of 1,5-dibenzyl-1H-pyrazolo[3,4-d]pyrimidine-4(5H)-thione "MF1" was estimated on the corrosion of mild steel in 1.0 M HCl solution using weight loss, Electrochemical Impedance Spectroscopy (EIS), Tafel polarization curves and theoretical calculation methods. The results of the polarization curves show that the corrosion current density decreases 577.9 $\mu\text{A}/\text{cm}^2$ to 38.5 $\mu\text{A}/\text{cm}^2$ after addition of the inhibitor. The charge transfer resistance increases 21.08 $\text{ohm}\cdot\text{cm}^2$ to 402.2 $\text{ohm}\cdot\text{cm}^2$ in the electrochemical impedance spectrum after addition of the inhibitor. Potentiodynamic polarization curves show that 1,5-dibenzyl-1H-pyrazolo[3,4-d]pyrimidine-4(5H)-thione act as mixed type inhibitor. The adsorption of inhibitors obeys the Langmuir adsorption isotherm, and the thermodynamic parameters (E_w , K_{ads} , ΔG^0_{ads}) were calculated and discussed. Quantum chemical calculations showed that the inhibitor has the tendency to be protonated in the acid and the results agree with experimental observations.

Key words: corrosion, inhibition, mild steel, 1,5-dibenzyl-1H-pyrazolo[3,4-d]pyrimidine-4(5H)-thione, electrochemical system, HCl 1M, DFT.

INTRODUCTION

Acid solutions are generally used for removal of undesirable scale and rust on the metals, cleaning of boilers and heat exchangers, oil-well acidizing in oil recovery, and so on. [1–4]. HCl solution is one of the most widely used agents for these goals. However, iron and its alloys could be corroded during these applications which result in a waste of resources. Corrosion prevention systems favor the use of chemicals with low or no environmental impacts.

The reduction in the corrosion rate of metals has numerous advantages such as saving of resources, economic benefits during the industrial applications, increasing the lifetime of equipment and decreasing the dissolution of toxic metals from the components into the environment. Therefore, the prevention of metals against corrosion is vital and must be dealt with. Commercial inhibitors are generally inorganic and some kind of organic compounds. However, the usage of some of them has been restricted due to the toxicity of their insufficient inhibitory efficiencies at low dosages [5–7]. In recent years, considerable amount of efforts have been devoted to find novel, healthy and efficient corrosion inhibitors. The use of organic inhibitors is one of the most practical methods for protection of metals against corrosion, and is becoming increasingly popular according to recent studies.

The existing data show that organic inhibitors act by adsorption and a film formation on the surface of metals. The adsorption of organic inhibitors on the metal surface can change the corrosion resistance properties of metals. Earlier studies have shown that organic compounds bearing heteroatoms with high electron density such as phosphorus, sulfur, nitrogen, oxygen or those containing multiple bonds, which are considered as adsorption centers, are effective inhibitors for the corrosion of metals [8–15]. The organic inhibitors are generally adsorbed on the metal surface through physical adsorption or chemical adsorption, which reduce the reaction area susceptible to corrosive attack [16–18].

MATERIALS AND METHODS

2.1. Inhibitors

1,5-dibenzyl-1H-pyrazolo[3,4-d]pyrimidine-4(5H)-thione was dissolved in the blank medium HCl 1M ranging the concentrations from 10^{-3} M to 10^{-6} M.

• Synthesis and crystallization

3.32 g (10 mmol) of 1,5-dibenzyl-1H, 4H, 5H-pyrazolo [3,4-d] pyrimidin-4-one is refluxed in pyridine (30 ml) with 5.55 g (25 mmol) of phosphorus pentasulfide for 4 h. Then the solvent was evaporated under reduced pressure. The precipitate that formed was washed with hot water to remove residual dimerized P_2S_5 until colourless filtrate was noted. The solid was re-crystallized from ethanol to afford the title compound as yellow crystals (yield: 85%; m.p. = 563 K) [19–21].

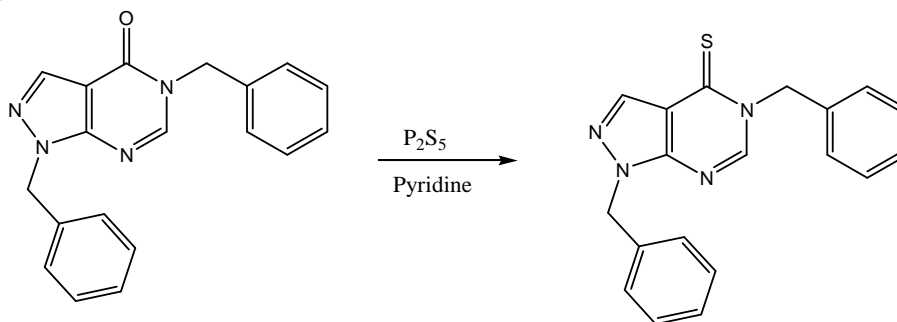


Figure 1: 1,5-dibenzyl-1H-pyrazolo[3,4-d]pyrimidine-4(5H)-thione

• Identification

Yield = 85%; mp: 160°C. 1H NMR (DMSO- d_6) δ ppm: 3.25 (2H, s, CH₂); 3.78 (2H, s, CH₂); 6.85–7.12 (q, 10H, Ar); 8.21 (1H, s, CH), 8.89 (1H, s, CH). ^{13}C NMR (DMSO- d_6) δ ppm: 51.83 (CH₂); 54.31 (CH₂); 118.24; 127.94 (Cq); 128.11–137.89 (CHAr); 145.54 (CH); 150.95 (CH); 179.82 (Cq, C=S). HRM (ESI) [M + H]: m/z = 310.

2.2. Materials

Tests were performed on a cold rolled steel (CRS) of the following composition (0.09% P; 0.38% Si; 0.01% Al; 0.05% Mn; 0.21% C; 0.05% S and the remainder iron) were polished with emery paper up to 1200 grade, washed thoroughly with double-distilled water, degreased with AR grade ethanol, acetone and dried at room temperature. MS samples of size 1.0 x 1.0 x 1.0 cm and MS powder were used for weight loss studies. For electrochemical studies, specimens with an exposed area of 1 cm² were used. These specimens were degreased ultrasonically with 2-propanol and polished mechanically with different grades of emery paper to obtain very smooth surface.

2.3. Solution

The test solutions were prepared by the dilution of analytical grade 37 % HCl with distilled water up to the optimum inhibitor concentration of “MF1”. For pH studies, the test solutions were prepared by the dilution of distilled water up to the optimum concentration, which was reached by adjusting the pH using HCl and NaOH. Inhibitor was dissolved in acid solution at required concentrations in (Mol/L) and the solution in the absence of inhibitor was taken as blank for comparison purposes. The test solutions were freshly prepared before each experiment by adding “MF1” directly to the corrosive solution. Experiments were conducted on several occasions to ensure reproducibility. Concentrations of “MF1” were 10^{-6} , 10^{-5} , 10^{-4} and 10^{-3} Mol/L.

RESULTS AND DISCUSSION

3.1. Weight loss measurements

The gravimetric method (weight loss, wL) is known to be the most widely used method of monitoring inhibition efficiency [22–25]. The mild steel specimens of dimension 1 x 1 x 0.1 cm were used in these studies. The weight

loss measurements were conducted under total immersion using 250 mL capacity beakers containing 100 mL of test solutions, HCl 1M solution containing the inhibitor “MF1” at different concentrations, for 6 hours, maintained in a thermostated water bath. Immersion is subjected to a temperature of 308 ° K to 6 hours. The specimens were weighed before and after the tests using an analytical balance with a precision of 0.1 mg. The specimens were taken out after the 6 hours of immersion, washed, dried and reweighed accurately to determine the weight loss of mild steel. All measurements were performed few times and average values were reported to obtain good reproducibility. The corrosion rate (ρ) in $\text{mg cm}^{-2} \text{h}^{-1}$ in the absence and presence of “MF1” was determined using the following equation:

$$\rho = \frac{\Delta W}{A t} \quad (1)$$

where ΔW is the average weight loss of the mild steel specimens, A is the total area of mild steel specimen and t is the immersion time. The percentage inhibition efficiency (IE%) was calculated using the relationship:

$$\text{IE (\%)} = \frac{W_0 - W_i}{W_0} \times 100 \quad (2)$$

where W_0 and W_i are the weight loss values in the absence and presence of “MF1”.

Table 1 listed the corrosion rate values and the efficiencies of the inhibitions for “MF1”, it is clear that “MF1” showed a best inhibitive effect, the efficiency reach until 95.8 % in HCl1M medium. This result could be explain by the presence of molecular structure containing heteroatoms having higher basicity and electron density on the hetero atoms such as N and substituents have tendency to resist corrosion.

Table 1. weight loss measurements of different concentration with and without presence of “MF1” in HCl 1M medium

Compounds	C	Corrosion rate (mg/cm ² .h)	Efficiencies %
Blank	1M	0.32	–
Inhibitor “MF1”	10 ⁻⁶	0.0461	85.58
	10 ⁻⁵	0.0319	90.04
	10 ⁻⁴	0.0205	93.59
	10 ⁻³	0.0134	95.8

2.4. Adsorption isotherm

Metal Surface providing us several information about the adsorption mechanism of the inhibitors on the surface by studying the relationship between the concentration and the surface coverage. Many isotherms are employed to fit the experimental data such as Langmuir, Temkin, Frumkin etc...

It is found that the adsorption of studied inhibitors on steel surface obeys the Langmuir adsorption isotherm equation:

$$\frac{C}{\theta} = \frac{1}{K} + C \quad (3)$$

Where C is the concentration of inhibitor, K the adsorption equilibrium constant, and θ is the surface coverage. Plots of C/θ against C yield straight lines as shown in Fig. 2, and the corresponding linear regression parameters are listed in Table 2. These parameters indicating the adsorption of “MF1” inhibitor on steel surface obeys Langmuir adsorption isotherm.

Furthermore, the adsorption equilibrium constant (K) is related to the standard free energy ΔG° by the following equation:

$$\Delta G^\circ_{ads} = -RT \cdot \ln(55.5 \cdot K) \quad (4)$$

Where R is the gas constant (8.314 J K⁻¹ mol⁻¹), T the absolute temperature(K), and the value 55.5 is the concentration of water in the solution.

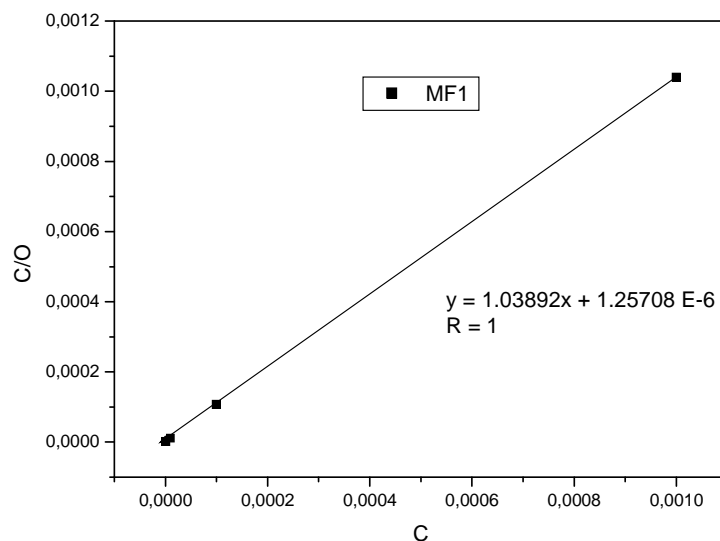


Fig.2.Langmuir adsorption of “MF1” on the mild steel in HCl 1M medium

Table 2 :Thermodynamics parameters adsorption of inhibitors on the steel mild in HCl 1M media

Measurements	Inhibitor	K_{ads} L mol ⁻¹	ΔG_{ads}° kJ mol ⁻¹	Linear coefficient regression (r)
Weightloss	“MF1”	$7.95 \cdot 10^5$	-8.637	1

The table 2 represent the ΔG_{ads}° values, the negative values of the free energy means that the inhibitor was spontaneously adsorbed on mild steel–electrolyte interface. It has been reported that values of ΔG_{ads}° up to -20 kJ/mol are consistent with the physisorption; those around -40 kJ/mol or higher are consistent with chemisorptions [26]. In the present study, the value of ΔG_{ads}° is -8.637 kJ mol⁻¹, probably means that the adsorption of 1,5-dibenzyl-1H-pyrazolo[3,4-d]pyrimidine-4(5H)-thione on the steel surface exhibits is physical adsorption.

3.3 Electrochemical measurements

The EIS is a method designed to avoid severe deterioration of the exposed surface of the structure studied and was widely used for monitoring the corrosion of a working electrode. This method consists of applying frequencies and low amplitude sinusoidal voltage wave to produce perturbation signals on the working electrode. The corrosion state can be predicted by analyzing the current response of the voltage or the frequencies. In modern practice, the impedance is usually measured with lock-in amplifiers or frequency-response analyzers, which are faster and more convenient than impedance bridges [27, 28].

The electrolysis cell was Pyrex of cylinder closed by cap containing five openings. Three of them were used for the electrodes. The working electrode was mild steel with the surface area of 1 cm². Before each experiment, the electrode was polished using emery paper until 1200 grade. After this, the electrode was cleaned ultrasonically with distillate water. A saturated calomel electrode (SCE) was used as a reference. All potentials were given with reference to this electrode. The counter electrode was a platinum plate of surface area of 1 cm². The temperature was thermostatically controlled at 308 K°. The working electrode was immersed in test solution during 30 minutes until a steady state open circuit potential (E_{ocp}) was obtained. The polarization curve was recorded by polarization from -800 mV to -200 mV under potentiodynamic conditions corresponding to 1mV/s (sweep rate) and under air atmosphere.

The potentiodynamic measurements were carried out using VoltaLab100 electrochemical analyzer, which was controlled by a personal computer. AC-impedance studies also were carried out in a three electrode cell assembly. The data were analyzed using Voltmaster 4.0 software. The electrochemical impedance spectra (EIS) were acquired in the frequency range 100 kHz to 10 mHz at the free corrosion potential. The charge transfer resistance (R_{ct}) and double layer capacitance (C_{dl}) were determined from Nyquist plots. The impedance diagrams are given in the Nyquist representation. Experiments are repeated three times to ensure the reproducibility. All electrochemical studies were carried out with immersion time of 1 hour, with different inhibitory concentrations of “MF1”, at 308 K.

3.3.1. Electrochemical impedance measurements

EIS was carried out on a newly polished steel surface in acidic solution in the absence and presence of inhibitor at an open circuit potential at 308 K° after 30 min of immersion.

The locus of the Nyquist plots was regarded as one part of a semicircle. Nyquist plots of steel in inhibited and uninhibited acidic solution containing various concentrations of “MF1” are shown respectively in Fig. 3.

The impedance diagrams obtained are not perfect semicircles and this difference has been attributed to frequency dispersion [29-30]. It is noteworthy that the best fit of the experimental data was obtained using constant phase elements (CPE) which have frequency dispersion rather than capacitances. Based on the values of the electric elements and parameters obtained in them, capacitances were assessed in accordance with the method described by Hsu and Mansfeld [31]. CPE is a generalized tool, which can reflect exponential distribution of the parameters of the electrochemical reaction related to energetic barrier at charge and mass transfer, as well as impedance behaviour caused by fractal surface structure. On the other hand there are some cases where the CPE is a formal approximation of the system, having very complicated parameter distribution and it is not possible to give some consistent physical interpretation [30]. The dispersion of the capacitive semicircle is explained also by surface heterogeneity due to surface roughness, impurities or dislocations [30-32].

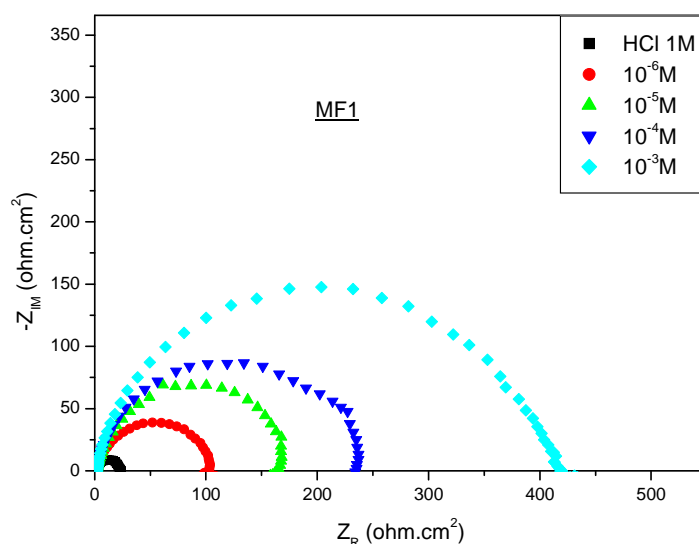


Figure 3. Nyquist plots in absence and presence of different concentrations of “MF1” in HCl 1M

The charge transfer resistance, R_t values are calculated from the difference in impedance at lower and higher frequencies, as suggested by Tsuru *et al.* [33]. To obtain the double layer capacitance (C_{dl}), the frequency at which the imaginary component of the impedance is maximum ($-Z_{max}$) is found and C_{dl} values are obtained from the equation:

$$C_{dl} = \frac{1}{2\pi \cdot f_{max} \cdot R_{ct}} \quad (5)$$

The percentage inhibition efficiency from the charge transfer resistance is calculated by the following relation:

$$E (\%) = \frac{R^{o\text{corr}} - R_{\text{corr}}}{R^{o\text{corr}}} \times 100 \quad (6)$$

where, $R^{o\text{corr}}$ and R_{corr} are the charge transfer resistance in presence and in absence of inhibitors, respectively.

The impedance parameters derived from these investigations are given in Table 3. It is found that R_t values increase with the increase in 1,5-dibenzyl-1H-pyrazolo[3,4-d]pyrimidine-4(5H)-thione concentration indicating an insulated adsorption layer's formation.

The double layer capacitance C_{dl} is expressed in the Helmutz model by:

$$C_{dl} = \frac{\epsilon_0 \epsilon S}{\delta} \quad (7)$$

Where δ is the thickness of the deposit, S is the surface of the electrode, ϵ_0 is the permittivity of the air and ϵ is the medium dielectric constant. The decrease in C_{dl} values may be interpreted either by a decrease of local dielectric constant ϵ [34] or by the thickness of the adsorbate layer of inhibitor at the metal surface [35].

Table. 3. Corrosion parameters obtained by impedance measurements for mild steel in HCl 1M at various concentrations of “MF1”

Compounds	Concentrations (M)	R_{ct} (ohm.cm ²)	f_{max} (Hz)	C_{dl} (μ F/cm ²)	E (%)
Blank	HCl 1M	21.08	100	75.5	-
Inhibitor “MF1”	10^{-6}	105.8	40	37.6	80.07
	10^{-5}	176.3	40	22.56	88.04
	10^{-4}	246.5	31.6	20.43	91.45
	10^{-3}	402.2	20	19.78	94.76

From Table 3, it is clear that the R_{ct} values increased and that the C_{dl} values decreased with increasing inhibitor concentration. These results indicate a decrease in the active surface area caused by the adsorption of the inhibitors on the mild steel surface, and it suggests that the corrosion process became hindered. The best result for the inhibition efficiency of the MF1 was obtained at a concentration of 10^{-3} Mol/L, with efficiency equal to 94.76 %.

3.3.2. Polarisation measurements

The polarization curves of steel in HCl 1M in the absence and presence of “MF1” at different concentrations at 308 K are presented in Fig. 4. The collected parameters deduced from the polarization curves such the corrosion potential (E_{corr}), corrosion current (I_{corr}), cathodic Tafel slopes (β_c) and percentage inhibition efficiency (EI %) are shown in Table 4. The relation determines the inhibition efficiency (EI %):

$$E(\%) = \frac{I^{\circ}corr - I_{corr}}{I^{\circ}corr} \times 100 \quad (8)$$

Where I°_{corr} and I_{corr} are uninhibited and inhibited corrosion current densities, respectively. Under the experimental conditions performed, the cathodic branch represents the hydrogen evolution reaction, while the anodic branch represents the iron dissolution reaction.

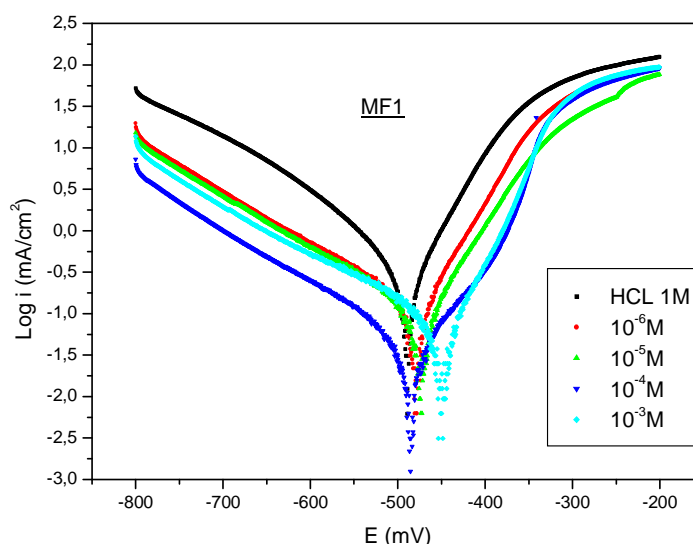


Fig.4. Tafel polarization curves in in HCl 1M with and without “MF1” at different concentrations

Table 4. Electrochemical parameters of mild steel at various concentrations of “MF1” HCl (1M)

Compounds	Concentration (M)	-E _{Corr} (mV)	β _c (mV/dec)	β _a (mV/dec)	I _{Corr} (mA/cm ²)	E (%)
Blank	HCL 1M	490	-147.7	74.8	0.5779	-
Inhibitor “MF1”	10 ⁻⁶	479	-166.5	61.6	0.132	77
	10 ⁻⁵	474	-150.9	64.4	0.087	85
	10 ⁻⁴	485	-169.2	60.5	0.0511	91
	10 ⁻³	452	-141.1	51.7	0.0385	93

Inspection of these results reveal that in presence of inhibitor (“MF1”), the value of corrosion density (I_{corr}) was decreased. This behaviour reflects its ability to inhibit the corrosion of mild steel in 1M HCl solution. Both the anodic and cathodic current densities were decreased in figure 4, indicating that “MF1” suppressed both the anodic and cathodic reactions through adsorption on the mild steel surface. This suggests that “MF1” act as mixed type corrosion inhibitor for mild steel in 1M HCl solution. Generally, the modes of the inhibition effect of inhibitors are classified into three categories [36,37]: geometric blocking effect of adsorbed inhibitive species, active sites blocking effect by adsorbed inhibitive species, and electro catalytic effect of the inhibitor or its reaction products. It has been discussed in the case of the first mode that inhibition effect comes from the reduction of the reaction area on the surface of the corroding metal, whereas for the other two modes the inhibition effects are due to the changes in the average activation energy barriers of the anodic and cathodic reactions of the corrosion process.

The cathodic Tafel slope (β_c) of “MF1” show changes with the addition of inhibitor, which suggests that the inhibiting action occurred by simple blocking of the available cathodic sites on the metal surface, which lead to a decrease in the exposed area necessary for hydrogen evolution and lowered the dissolution rate with increasing the inhibitors concentrations (table 4). The parallel cathodic Tafel plots of “MF1” obtained in Figure 4 indicate that the hydrogen evolution is activation controlled and the reduction mechanism is not affected by the presence of inhibitors [38-40].

Tafel slopes of β_c and β_a change upon addition of “MF1”, which means that the inhibitor molecules are adsorbed on both the anodic and cathodic sites resulting in an inhibition of both anodic dissolution and cathodic reduction reactions [41].

3.4. Effect of temperature

Temperature has a great effect on the corrosion phenomenon. Generally the corrosion rate increases with the rise of the temperature. For this purpose, we made weight loss experiments in the range of temperature 318–348K, in the absence and presence of 1,5-dibenzyl-1H-pyrazolo[3,4-d]pyrimidine-4(5H)-thione after 1 h of immersion at optimum concentration (10⁻³ Mol/L). The corresponding data are shown in Table 5, Figure 5. From the weight loss results, the corrosion rate (CR), the inhibition efficiency (E%) of inhibitors and degree of surface coverage (θ) were calculated using equations 9, 10 and 11 [42]:

$$CR = \left(\frac{\Delta W}{Sxt} \right) \quad (9)$$

$$E(\%) = \left(1 - \frac{W_{corr}}{W_{corr}^o} \right) \times 100 \quad (10)$$

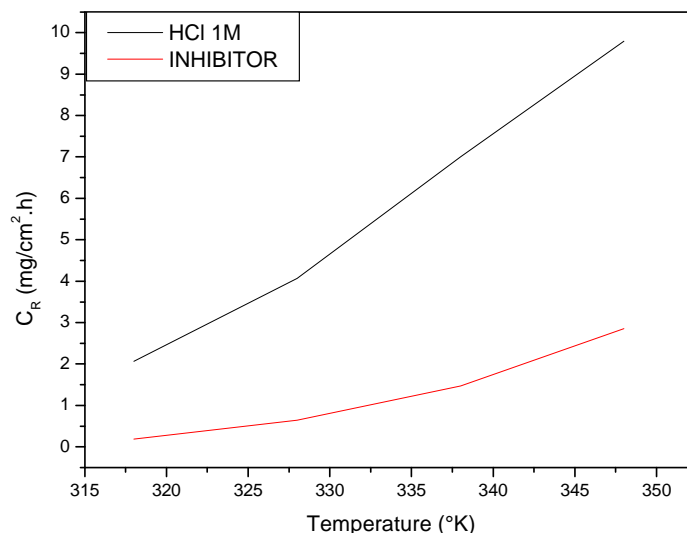
$$\theta = \left(1 - \frac{W_{corr}}{W_{corr}^o} \right) \quad (11)$$

Where W_{corr} and W_{corr}^o are the weight losses for mild steel in the presence and absence of the inhibitor in HCl solution and θ is the degree of surface coverage of the inhibitors. ΔW is the difference of weight loss for mild steel with and without inhibitors, S is the exposure area of the metallic specimens and t is the immersion time of the metal in corrosive solution.

The fractional surface coverage (θ) can be easily determined from the weight loss measurements by the ratio E(%)/100, where E(%) is inhibition efficiency and calculated using equation 10. The data obtained suggest that 1,5-dibenzyl-1H-pyrazolo[3,4-d]pyrimidine-4(5H)-thione get adsorbed on the steel surface at all temperatures studied and corrosion rates increased in absence and presence of inhibitor with increase in temperature in HCl 1M solutions. In acidic media, corrosion of metal is generally accompanied with evolution of H₂ gas; rise in temperature usually accelerates the corrosion reactions which results in higher dissolution rate of the metal.

Table 5. Corrosion parameters for mild steel in HCL 1M in absence and presence of optimum concentration of 1,5-dibenzyl-1H-pyrazolo[3,4-d]pyrimidine-4(5H)-thioneat different temperatures

Temperature (K ^o)	Inhibitor	C _R (mg/cm ² .h)	Θ	E (%)
318	HCL 1M	2.0649	---	---
	Inhibitor	0.192	0.9	90.7
328	HCL 1M	4.0689	---	---
	Inhibitor	0.6425	0.84	84.21
338	HCL 1M	6.9998	---	---
	Inhibitor	1.4692	0.79	79.01
348	HCL 1M	9.7914	---	---
	Inhibitor	2.8522	0.7	70.87

**Figure 5. Variation of CR in 1M HCl on steel surface without and with of optimum concentration of 1,5-dibenzyl-1H-pyrazolo[3,4-d]pyrimidine-4(5H)-thione at different temperatures**

From the Table 5, it is clear that corrosion rate increased with increasing temperature both uninhibited and inhibited solutions while the inhibition efficiency of 1,5-dibenzyl-1H-pyrazolo[3,4-d]pyrimidine-4(5H)-thione decreased with temperature. A decrease in inhibition efficiencies with the increase temperature in presence of the inhibitor might be due to weakening of physical adsorption. In order to calculate activation parameters for the corrosion process, Arrhenius equation (12) and transition state equation (13) were used [43].

$$CR = A \exp\left(\frac{-E_a}{R \times T}\right) \quad (12)$$

$$CR = \frac{R \times T}{N \times h} \exp\left(\frac{-\Delta S_a}{R}\right) \exp\left(\frac{-\Delta H_a}{R \times T}\right) \quad (13)$$

where CR is the corrosion rate, R the gas constant, T the absolute temperature, A the pre-exponential factor, h the Planck's constant and N is Avogadro's number, E_a the activation energy for corrosion process, ΔH_a the enthalpy of activation and ΔS_a the entropy of activation. The apparent activation energy (E_a) at optimum concentration of 1,5-dibenzyl-1H-pyrazolo[3,4-d]pyrimidine-4(5H)-thione was determined by linear regression between Ln(CR) and 1/T (Figure 6) and the result is shown in Table 6.

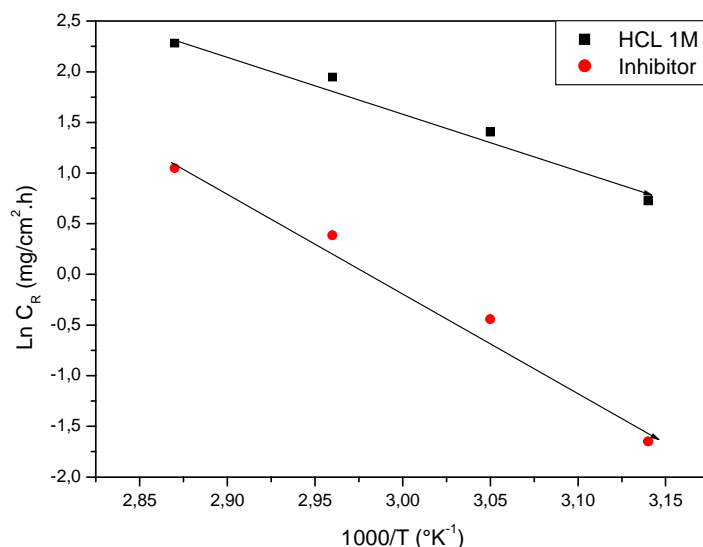


Figure 6. Arrhenius plots of $\ln CR$ vs. $1/T$ for mild steel in 1M HCl in the absence and the presence of 1,5-dibenzyl-1H-pyrazolo[3,4-d]pyrimidine-4(5H)-thione at optimum concentration (10^{-3} Mol/L)

Table 6. Activation parameters E_a , ΔH_a and ΔS_a for the mild steel dissolution in 1M HCl in the absence and the presence of 1,5-dibenzyl-1H-pyrazolo[3,4-d]pyrimidine-4(5H)-thione at optimum concentration (10^{-3} Mol/L)

Inhibitor	E_a (J/mol)	ΔH_a (KJ/mol)	ΔS_a (J/mol.K)
1M HCL	48.13	45.61	-95.79
Inhibitor	82.37	80	-7.18

Inspection of Table 6 showed that the value of E_a determined in 1M HCl containing 1,5-dibenzyl-1H-pyrazolo[3,4-d]pyrimidine-4(5H)-thione is higher (82.37 J/mol) than that for uninhibited solution (48.13 J/mol). The increase in the apparent activation energy may be interpreted as physical adsorption that occurs in the first stage. The increase in activation energy could be attributed to an appreciable decrease in the adsorption of the inhibitor on the steel surface with increase in temperature. As adsorption decreases more desorption of inhibitor occurs because these two opposite processes are in equilibrium. Due to more desorption of inhibitor molecules at higher temperatures the greater surface area of steel comes in contact with the aggressive environment, resulting in increased corrosion rates with increase in temperature [44-50].

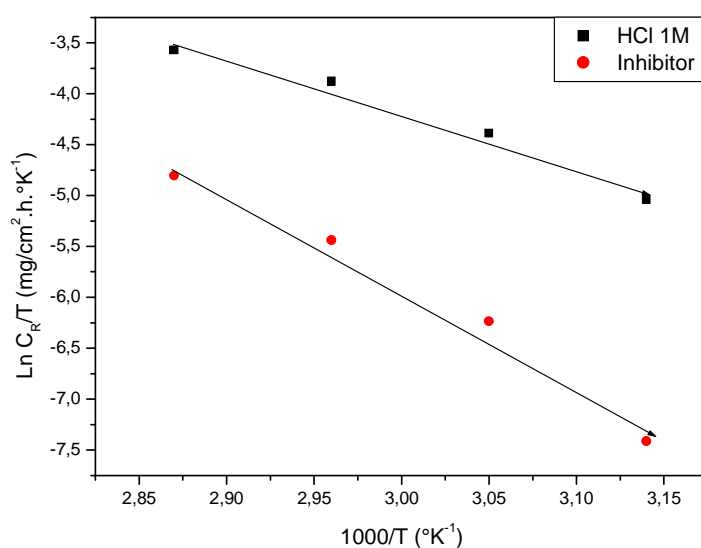


Figure 7. Arrhenius plots of $\ln CR/T$ vs. $1/T$ for steel in 1M HCl in the absence and the presence of 1,5-dibenzyl-1H-pyrazolo[3,4-d]pyrimidine-4(5H)-thione at optimum concentration (10^{-3} Mol/L)

Fig.7 showed a plot of $\ln CR/T$ versus $1/T$. The straight lines are obtained with a slope ($\Delta H_a/R$) and an intercept of $(\ln R/Nh + \Delta S_a / R)$ from which the values of the values of ΔH_a and ΔS_a are recalculated for 1,5-dibenzyl-1H-pyrazolo[3,4-d]pyrimidine-4(5H)-thione of analyzed and are given in Table 6. Inspection of these data revealed that the thermodynamic parameter (ΔH_a) for dissolution reaction of steel in 1M HCl in the presence of inhibitors are higher (80 kJ/mol) than that of in the absence of inhibitors (45.61 kJ/ mol). The positive sign of ΔH_a reflect the endothermic nature of the steel dissolution process suggesting that the dissolution of steel is slow in the presence of inhibitor. Negative value of entropy (ΔS_a) imply that the activated complex in the rate determining step represents an association rather than a dissociation step, meaning that a decrease in disordering takes place on going from reactant to the activated complex.

3.5. Quantum chemical calculations

Quantum chemical calculations can complement the experimental investigations or even predict with some confidence into experimentally unknown properties [51, 52]. There has been increasing use of the density functional theory (DFT) methods in applications related to organic compounds [53].

The advancement in methodology and implementations has reached a point where predicted properties of reasonable accuracy can be obtained from DFT calculations [54]. Thus in the present investigation quantum chemical calculation using DFT was employed to explain the experimental results obtained in this study and to further give insight into the inhibition action of “MF1” on the mild steel surface.

Complete geometrical optimizations of the investigated molecules are performed using DFT (density functional theory) with the Beck’s three parameter exchange functional along with the Lee–Yang–Parr nonlocal correlation functional (B3LYP) [55–57] with 6-31G(d,p) basis set is implemented in Gaussian 03 program package [58]. This approach is shown to yield favorable geometries for a wide variety of systems. This basis set gives good geometry optimizations. The geometry structure was optimized under no constraint. The aim of our calculation is to calculate the following quantum chemical indices: The energy of highest occupied molecular orbital (E_{HOMO}), the energy of lowest unoccupied molecular orbital (E_{LUMO}), energy gap (ΔE) between E_{HOMO} and E_{LUMO} , dipole moment (μ), electronegativity (χ), electron affinity (A), global hardness (η), softness (σ), ionization potential (I), the global electrophilicity (ω), the fraction of electrons transferred (ΔN) and the total energy (TE), and correlate these with the experimental observations. The optimized structures of MF1 and N-MF1 are depicted in Fig 8 which is shown below.



Fig 8. Optimized structure of studied molecules obtained by B3LYP/6-31G(d,p) level

The frontier orbital (highest occupied molecular orbital HOMO and lowest unoccupied molecular orbital LUMO) of a chemical species are very important in defining its reactivity. Fukui first recognized this. A good correlation has been found between the speeds of corrosion and E_{HOMO} that is often associated with the electron donating ability of the molecule. Survey of literature shows that the adsorption of the inhibitor on the metal surface can occur on the basis of donor–acceptor interactions between the π -electrons of the heterocyclic compound and the vacant d-orbital of the metal surface atoms [59], high value of E_{HOMO} of the molecules shows its tendency to donate electrons to appropriate acceptor molecules with low energy empty molecular orbitals. Increasing values of E_{HOMO} facilitate adsorption and therefore enhance the inhibition efficiency, by influencing the transport process through the adsorbed layer. Similar relations were found between the rates of corrosion and ΔE ($\Delta E = E_{LUMO} - E_{HOMO}$) [60–61]. The energy of the lowest unoccupied molecular orbital indicates the ability of the molecule to accept electrons. The lower the value of E_{LUMO} , the more probable the molecule would accept electrons. Consequently, concerning the value of the energy gap ΔE , larger values of the energy difference will provide low reactivity to a chemical species. Lower values of the ΔE will render good inhibition efficiency, because the energy required to remove an electron from the lowest occupied orbital will be low [62]. Another method to correlate inhibition efficiency with parameters of molecular structure is to calculate the fraction of electrons transferred from inhibitor to metal surface. According

to Koopman's theorem [63], EHOMO and ELUMO of the inhibitor molecule are related to the ionization potential (I) and the electron affinity (A), respectively. The ionization potential and the electron affinity are defined as $I = -EHOMO$ and $A = -ELUMO$, respectively. Then absolute electronegativity (χ) and global hardness (η) of the inhibitor molecule are approximated as follows [64]:

$$\chi = (I+A)/2 \quad (14)$$

$$\eta = (I-A)/2 \quad (15)$$

The global electrophilicity index was introduced by Parr [65] and is given by:

$$\omega = \mu^2 / 2\eta \quad (16)$$

Moreover, for a reaction of two systems with different electronegativities, the electronic flow will occur from the molecule with the lower electronegativity (the organic inhibitor) towards that of higher value (metallic surface), till the chemical potentials are equal [66]. Therefore the fraction of electrons transferred (ΔN) from the inhibitor molecule to the metallic atom was calculated according to Pearson electronegativity scale [67]:

$$\Delta N = (\chi_{Fe} - \chi_{inh}) / 2(\eta_{Fe} - \eta_{inh}) \quad (17)$$

Where χ_{Fe} and χ_{inh} denote the absolute electronegativity of Fe and the inhibitor molecule, respectively; η_{Fe} and η_{inh} denote the absolute hardness of Fe and the inhibitor molecule, respectively. A theoretical value for the electronegativity of bulk iron was used $\chi_{Fe} = 7$ eV and a global hardness of $\eta_{Fe} = 0$, by assuming that for a metallic bulk $I = A$ because they are softer than the neutral metallic atoms [68].

Quantum chemical parameters obtained from the calculations which are responsible for the inhibition efficiency of inhibitors, such as the highest occupied molecular orbital (E_{HOMO}), energy of lowest unoccupied molecular orbital (E_{LUMO}), HOMO-LUMO energy gap (ΔE_{H-L}), dipole moment (μ) and total energy (TE), electronegativity (χ), electron affinity (A), global hardness (η), softness (σ), ionization potential (I), The global electrophilicity (ω), the fraction of electrons transferred from the inhibitor to iron surface (ΔN) and the total energy (TE), are collected in Table 7.

Table.7. Calculated quantum chemical parameters of the studied compounds

Quantum parameters	MF1	N-MF1
E_{HOMO} (eV)	-0.276	-0.218
E_{LUMO} (eV)	-0.042	-0.038
ΔE_{gap} (eV)	0.234	0.180
Dipole moment μ (debye)	3.3523	7.0191
Total energy (a.u.)	0.757085	1.0701
Ionisation potential ($I = -E_{HOMO}$)	0.276	0.218
Electron affinity ($A = -E_{LUMO}$)	0.042	0.042
Hardness ($\eta = (I-A)/2$ (eV))	0.117	0.088
Softness ($\sigma = 1/\eta$)	8.547	11.363
Electronegativity ($\chi = (I+A)/2$ (eV))	0.297	0.239
Electrophilicity index ($\omega = \mu^2/2\eta$)	48.025	279.930
Fractions of electron transferred ($\Delta N = (\chi_{Fe} - \chi_{inh})/2(\eta_{Fe} - \eta_{inh})$)	0.02157	0.01728

The results presented in Table 7 show that N-MF1 (protonated) have the lowest energy gap 0.180eV, therefore, its high reactivity can allow it to be easily adsorbed onto the mild steel surface leading to increase its inhibitive efficiency when compared to MF1.

The electronegativity and the global hardness indicate the molecular capability of accepting electrons then the smaller their values, the higher their ability of donating electrons. It could be seen from their calculated values shown in Table 7, that P2 have the lowest electronegativity and the lowest hardness values indicating the high reactivity of N-MF1 compared to MF1 which can explain its high corrosion inhibition efficiency.

The values of the dipole moment displayed in Table 7, are the measurement of polarity within the entire molecules [69]. It is an index usually used for the prediction of the direction of a corrosion inhibition. Hence, it is generally agreed that the adsorption of polar compounds possessing high dipole moments on the mild steel surface should lead to better inhibition efficiency [70].

The total energy calculated by quantum chemical methods is also a beneficial parameter. The total energy of a system is composed of the internal, potential, and kinetic energy. Hohenberg and Kohn [70] proved that the total energy of a system including that of the many body effects of electrons (exchange and correlation) in the presence of static external potential (for example, the atomic nuclei) is a unique functional of the charge density. The minimum value of the total energy functional is the ground state energy of the system. The electronic charge density which yields this minimum is then the exact single particle ground state energy. In our study the total energy of the best inhibitor MF1 is equal to 0.757085(u.a), this value is lower than that of the compound N-MF1.

In literature it has been reported that the values of ΔN show inhibition effect resulted from electrons donation [71, 72]. According to Lukovits's study [72], if the value of $\Delta N < 3.6$, the inhibition efficiency increased with increasing electron donating ability of inhibitor at the metal surface. Also it was observed [73] that inhibition efficiency increased with increase in the values of ΔN . However, our study reveals that there is no regular trend in the inhibition efficiency by increasing values of ΔN .

As we know, frontier orbital theory is useful in predicting the adsorption centres of the inhibitors responsible for the interaction with surface metal atoms. Fig 10, show the HOMO and LUMO orbital contributions for the studied inhibitor molecules MF1 and N-MF1 respectively. For all the molecules, the HOMO densities were concentrated on both rings, N atoms, and S-atom. This means that these are active sites of the molecules responsible for interaction with metal surface.

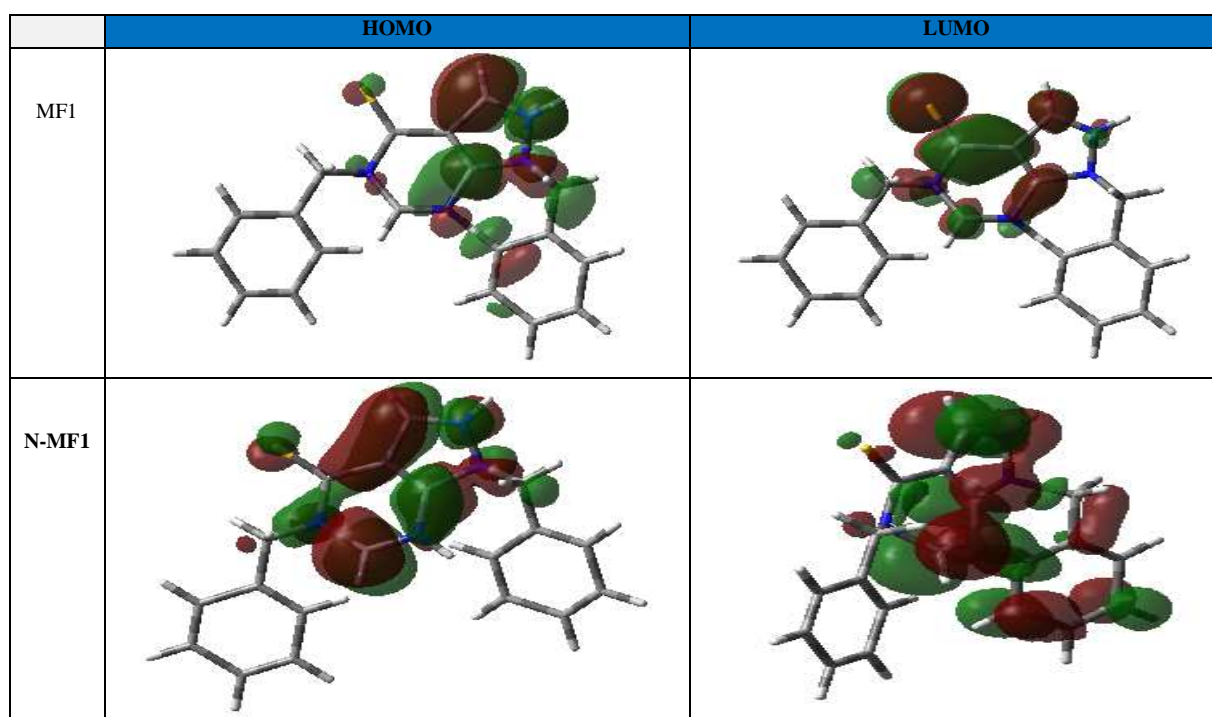


Fig.9. The frontier molecular orbital density distribution of MF1 and N-MF1

CONCLUSION

The principal finding of present work can be summarized as follows:

- Steady state electrochemical measurements have shown that 1,5-dibenzyl-1H-pyrazolo[3,4-d]pyrimidine-4(5H)-thione act as mixed inhibitor for the corrosion of steel in HCl 1M without modifying the mechanism of hydrogen evolution reaction.
- The increase in the charge transfer resistance and decrease in double layer capacitance values, with the increase in the inhibitor concentration, showed that 1,5-dibenzyl-1H-pyrazolo[3,4-d]pyrimidine-4(5H)-thione formed protective layers on the mild steel surface, covering areas where HCl solution degrades and corrodes rapidly.
- Inhibition efficiency increases with increase in the concentration of the inhibitor studied but decreases with rise in temperature.
- The corrosion process was inhibited by adsorption of the organic matter on the mild steel surface, obtaining the formation of the film on the metal/acid solution interface, decreasing the degradation of the material.

- Results obtained through weight loss measurements and electrochemical tests demonstrated that 1,5-dibenzyl-1H-pyrazolo[3,4-d]pyrimidine-4(5H)-thione act as efficient corrosion inhibitors of the mild steel in 1 M HCl solution..
- Through the quantum chemical calculations, we have shown that the calculated parameters are correlated with the experimental results, and it was found that inhibition effect increased with the lower ΔE_{gap} and the higher μ values. The protection ability of the MF1 can be attributed to its molecular protonated structure.

REFERENCES

- [1] A.G. Avdeev, Y.I. Kuznetsov, A.K. Buryak. *Corros. Sci.* **2013**, 69, 50–60.
- [2] P.B. Raja, A.K. Qureshi, A.A. Rahim, H. Osman, K. Awang. *Corros. Sci.* **2013**, 69, 292–301.
- [3] M. Yadav, S. Kumar, S.U. Sharma, P.N. Yadav. *J. Mater. Environ. Sci.* **2013**, 4 (5), 691–700.
- [4] G. Kardas. *Mater. Sci.* **2005**, 41, 337–343.
- [5] B. Qian, B. Hou, M. Zheng. *M. Corros. Sci.* **2013**, 72, 1–9.
- [6] N.A. Negm, N.G. Kandile, E.A. Badr, M.A. Mohammed. *Corros. Sci.* **2012**, 65, 94–103.
- [7] X. Li, S. Deng, H. Fu. *Corros. Sci.* **2012**, 62, 163–175.
- [8] R. Solmaz, E. Altunbas, G. Kardas, Prot. *Met. Phys. Met.* **2011**, 47, 262–269.
- [9] R. Solmaz, M.E. Mert, G. Kardas, B. Yazici, M. Erbil. *Acta Phys.- Chim. Sin.* **2008**, 24, 1185–1191.
- [10] A. Chetouani, A. Aouniti, B. Hammouti, N.B. Benchat, T. Benhadda, S. Kertit. *Corros. Sci.* **2003**, 45, 1675–1684.
- [11] M.A. Quraishi, J. Rawat. *Mater. Chem. Phys.* **2002**, 73, 118–122.
- [12] S.A. Abd El Maksoud. *Corros. Sci.* **2002**, 44, 803–813.
- [13] H. Elmsellem, H. Nacer, F. Halaimia, A. Aouniti, I. Lakehal, A. Chetouani, S. S. Al-Deyab, I. Warad, R. Touzani, B. Hammouti. *Int. J. Electrochem. Sci.* **2014**, 9, 5328.
- [14] M. Özcan, R. Solmaz, G. Kardas, I. Dehri. *Colloids Surf. A* **2008**, 325, 57–63.
- [15] H. Elmsellem, N. Basbas, A. Chetouani, A. Aouniti, S. Radi, M. Messali, B. Hammouti. *Portugaliae. Electrochimica. Acta*, **2014**, 2, 77.
- [16] IObot. I.B., Obi-Egbedi. N.O., Umoren. S.A., Antifungal drugs as corrosion inhibitors for aluminium in 0.1 M HCl. *Corros. Sci.* **2009**, 51, 1868–1875.
- [17] L. Fragoza-Mar, O. Olivares-Xometl, M.A. Domínguez-Aguilar, E.A. Flores, P. Arellanes-Lozada, F. Jiménez-Cruz. *Corros. Sci.* **2012**, 61, 171–184.
- [18] Solmaz. *R. Corrosion Science* **79 (2014)** 169–176.
- [19] M. El Fal, Y. Ramli, E.M. Essassi, M. Saad. & L. El Ammari. *Acta Cryst.* **2014**. **E70**, o1005–o1006.
- [20] M. El Fal, Y. Ramli, E.M. Essassi, M. Saadi & L. El Ammari. *Acta Cryst.* **2015**. **E71**, o95–o96.
- [21] M. El Fal, Y. Ramli, A. Zerzouf, A. Talbaoui, Y. Bakri, and E.M. Essassi. *Journal of Chemistry* **2015**, Article ID 982404, 6.
- [22] A. Bouyanzer, L. Majidi, B. Hammouti. *Bull. Electrochem.* **2006**; 22: 321.
- [23] Y. El ouadi, A. Bouyanzer, L. Majidi, J. Paolini, J.M. Desjobert, J. Costa, A. Chetouani, B. Hammouti, *Journal of Chemical and Pharmaceutical Research*, **2014**, 6(7):1401-1416.
- [24] Y. El Ouadi, A. Bouyanzer, L. Majidi, J. Paolini, J-M. Desjobert, J. Costa, A. Chetouani, Hammouti. B. Jodeh. S. Warad. I. Mabkhot. Y. BenHadda. T. Res *Chem Intermed DOI* 10.1007/s11164-014-1802-7.
- [25] M. Manssouri, Y. El Ouadi, M. Znini, J. Costa, A. Bouyanzer, J-M. Desjobert, L. Majidi. *Mater. Environ. Sci.* **2015**, 6 (3), 631-646.
- [26] F. Bentiss, M. Outirite, M. Traisnel, H. Vezin, M. Lagrenee, B. Hammouti, S.S. Al-Deyab et al., *Int. J. Electrochem. Sci.*, **2012**, 7: 1699-1723.
- [27] J. Kim, W. Lim, Y. Lee, S. Kim, S.R. Park, S.K. Suh, I. Moon, *Ind. Eng. Chem. Res.*, **2011**, 50, 8272.
- [28] M.A. Quraishi, A. Singh, V.K. Singh, Yadav. *Mater. Chem. Phys.* **2010**, 122, 114–122.
- [29] F. Mansfeld, M.W. Kending, S. Tsai. *Corrosion* **1982**, 38, 570.
- [30] Z.B., Stoynov, B.M. Grafov, B. Savova-Stoynova, V.V. Elkin, *Electrochemical Impedance, Nauka, Moscow*, 1991.
- [31] C.H. Hsu, F. Mansfeld, *Corrosion*, **2001**, 57, 747.
- [32] A. Popova, M. Christov. *Corrosion Science*, (2005).
- [33] T. Tsuru, S. Haruyama, B. Gijutsu, *J. Jpn. Soc. Corros. Eng.* **1978**, 27, 573.
- [34] E. McCafferty, N. Hackerman. *J. Electrochem. Soc.* **1972**, 119, 146.
- [35] J.M. Bastidas, J.L. Polo, E. Cano. *J. Appl. Electrochem.* **2000**, 30, 1173.
- [36] M. Znini, L. Majidi, A. Bouyanzer, J. Paolini, J.M. Desjobert, J. Costa, B. Hammouti, *Arab. J. Chem.* (2010), doi:10.1016/j.arabjc.2010.09.017
- [37] M. Znini, M. Bouklah, L. Majidi, S. Kharchouf, A. Aouniti, A. Bouyanzer, B. Hammouti, J. Costa, S.S. Al-Deyab. *Int. J. Electrochem. Sci.* **2011**, 6, 691.
- [38] I. Belfilali, A. Chetouani, B. Hammouti, A. Aouniti, S. Louhibi, S.S. Al-Deyab. *Int. J. Electrochem. Sci.* **2012**, 7(5), 3997.

- [39] A. Rochdi, O. Kassou, N. Dkhireche, R. Tourir, M. El Bakri, ME. Touhami, M. Sfaira, B. Mernari, B. Hammouti. *CorrosionScience* .**2014**, 80, 442.
- [40] H. Zarrok, A. Zarrouk, R. Salghi, B. Hammouti, M. Elbakri, ME. Touhami, F. Bentiss, H. Oudda. *Research on ChemicalIntermediates***2014**, 40, 801.
- [41] Li. Xianghong, ShuduanDeng , Hui Fu. *Corrosion Science*. **2011**, 53, 3704–3711.
- [42] M. Wang, J. Li, M. Rangarajan, Y. Shao. *LaVoie EJ, Huang TC, Ho CT. J. Agric. Food Chem.* **1998**, 46, 4869.
- [43] F. Togue-Kamga, BD. Btatkeu, C. Noubactep, P. Woaf. *Fresenius Environmental Bulletin*.**2012** , 21, 1992.
- [44] I. Belfilali, A. Chetouani, B. Hammouti, S. Louhibi, A. Aouniti, SS. Al-Deyab. *Research on ChemicalIntermediates*.**2014**, 40, 1069.
- [45] K. Bouhrira, A. Chetouani, D. Zerouali, B. Hammouti, A. Yahyi, A. Et-Touhami, R. Yahyaoui, R. Touzani. *Research on Chemical Intermediates*.**2014**, 40, 569.
- [46] A. Ousslim, K. Bekkouch, A. Chetouani, E. Abbaoui, B. Hammouti, A. Aouniti, A. Elidrissi, F. Bentiss. *Research on Chemical Intermediates*.**2014**, 40, 1201.
- [47] D. Bouzidi, A. Chetouani, B. Hammouti, S. Kertit, M. Taleb, SS. Al-Deyab. *International Journal of Electrochemical Science*. **2012**, 7, 2334.
- [48] D. Ben Hmamou, R. Salghi, A. Zarrouk, B. Hammouti, SS. Al-Deyab, L. Bazzi, H. Zarrok, A. Chakir, L. Bammou. *International Journal of Electrochemical Science*.**2012**, 7, 2361.
- [49] M. Abdallah, BH. Asghar, I. Zaaferany, A.S. Fouda. *International Journal of Electrochemical Science*.**2012**, 7, 282.
- [50] KF. Khaled. *Materials Chemistry and Physics*.**2008**, 112, 290.
- [51] E.E. Ebenso, O. Obot. *Ime. Int. J. Electrochem. Sci.*, **2010**, 5, 2012 – 20.
- [52] N. Khalil, *Electrochim. Acta*. **2003**, 48, 2635.
- [53] H. Elmsellem, A. Aouniti, M. Khoutoul, A. Chetouani, B. Hammouti, N. Benchat, Touzani. R., Elazzouzi. M.. *Journal of Chemical and Pharmaceutical Research*, **2014**, 6(4):1216-1224
- [54] C. Adamo, V. Barone. *Chem. Phys. Lett.* **2000**, 330, 152.
- [55] A. Zarrouk, B. Hammouti, R. Touzani, SS. Al-Deyab, M. Zertoubi, M., Dafali. A., Elkadiri. S., *Int. J. Electrochem.Sci.***2011**, 6, 4939.
- [56] A.D. Becke. *J. Chem. Phys.***1992**, 96, 9489.
- [57] A.D. Becke. *J. Chem. Phys.***1993**, 98, 1372.
- [58] C. Lee, W. Yang, R.G. Parr. *Phys. ReV. B*.**1998**, 37, 785.
- [59] A. Domenicano, I. Hargittai. *Oxford University Press, New York*, (**1992**).
- [60] W. Li, X. Zhao, F. Liu, J. Deng, B. Hou. *Mater. Corros.***2009**, 60, 287.
- [61] Hasanov. R., Sadikoglu. M., Bilgic. S., *Appl. Surf. Sci.*, 253 (2007) 3913.
- [62] Amin. M.A., Khaled. K.F., Fadl-Allah. S.A., *Corros. Sci.*, 52 (2010) 140.
- [63] H. Elmsellem, A. Aouniti, Y. Toubi, H. Steli, M. Elazzouzi, S. Radi, B. Elmahi, Y. El Ouadi, A. Chetouani, B. Hammouti, *Der. Pharma.Chemica*, **2015**, 7(7),353.
- [64] H. Wang, X. Wang, H. Wang, L. Wang, A. liu. *J. Mol. Model*.**2007**, 13, 147.
- [65] V.S. Sastri, J.R. Perumareddi, *Corrosion*.**1997**, 53, 671.
- [66] K.F. Khaled. *Electrochim.Acta*,**2010**, 22, 6523.
- [67] V.S. Sastri, J.R. Perumareddi. *Corrosion*, **1997**, 53, 617.
- [68] E.E. Ebenso, D.A. Isabiry. *Int. J. Mol. Sci.*, **2010**, 11, 2473.
- [69] I. Lukovits, E. Kalman, F. Zucchi. *Corrosion*,**2001**, 57, 3.
- [70] H. Ju, Z.P. Kai, Y. Li. *Corros. Sci.*, **2008**, 50, 865.
- [71] R.G. Pearson, *Inorg. Chem*.**1998**, 27, 734.
- [72] X. Li, S. Deng, H. Fu, T. Li. *Electrochim. Acta.*, **2009**, 54, 4089.
- [73] I. Lukovits, E. Kalman, F. Zucchi. *Corrosion.*,**2001**, 57, 3.